

# SURFACE-ENHANCED RAMAN SCATTERING OF BIOLOGICAL MOLECULES ON METAL COLLOIDS: BASIC STUDIES AND APPLICATIONS TO QUANTITATIVE ASSAY

Xiao-Ming Dou<sup>†+</sup> and Yukihiro Ozaki<sup>‡ 1</sup>

*\*Institute of Optics and Photoelectronics, Shanghai Jiao Tong University, Shanghai, 200030, China and <sup>†</sup>Basic Technology Research Laboratory, KDK Corporation, 57 Nishi Aketa-cho, Higashi Kujo, Minami-ku, Kyoto 601-8501, Japan; <sup>‡</sup>Department of Chemistry, School of Science, Kwansei-Gakuin University, Uegahara, Nishinomiya 662-8501, Japan*

## 1. INTRODUCTION

The history of surface-enhanced Raman scattering (SERS) stretches back more than twenty years.<sup>1-10</sup> The discovery of enormous enhancement of the Raman scattering from pyridine adsorbed on a roughened silver electrode has opened up a new field of surface spectroscopy. It is well known that the SERS intensity is emerged by resonance effects of the optical fields with the surface plasmons of the SERS-active substrate (electromagnetic enhancement) or the charge-transfer transition between metal and sample molecules (chemical enhancement).<sup>1-10</sup>

SERS has been applied extensively to various fields of science and technology including surface science, electrochemistry, and analytical chemistry.<sup>1-10</sup> Recently, the applications of SERS to trace assays in biological and medical problems have been matters of great interest since SERS holds considerable promise as a highly sensitive analytical tool. SERS has three major advantages for bioanalytical applications.<sup>3,5,6,8-10</sup> One is the very large enhancement of the Raman cross-section of the absorbed molecules by a factor of  $10^3$ - $10^9$ . The SERS effect becomes even more remarkable if the frequency of the excitation light is in resonance with a major absorption band

---

<sup>1</sup> Mailing address; Yukihiro Ozaki; Department of Chemistry, School of Science, Kwansei-Gakuin University, Uegahara, Nishinomiya 662-8501, Japan. Fax: 81-798-51-0914. E-mail: ozaki@kwansei.ac.jp

of the molecule being illuminated (surface-enhanced resonance Raman scattering; SERRS). Second, in SERS spectra there is a marked reduction in the fluorescence background which often obscures Raman scattering from biological molecules. The third is the surface selectively which SERS effect provides; only molecules on or very near the metal surface can contribute to the signal in SERS spectra.

SERS offers enormous potential for the studies of biological materials from small molecules to tissues. SERS-based bioanalytical applications include the following: (1) Microanalysis or trace analysis of simple biological compounds such as amino acids, nucleotides, and biological pigments.<sup>11-21</sup> Because of the very high sensitivity of SERS, one can obtain Raman spectra of biological molecules at concentrations down to  $\sim 10^{-12}$  M. (2) DNA gene probes, gene diagnosis, quantitative assay of double-stranded (ds)-DNA, and studies of antitumor drug target complexes.<sup>22-27</sup> (3) Assay of thiol groups.<sup>28</sup> (4) Enzyme immunoassay employing SERS.<sup>29-31</sup> (5) The SERS microprobe approach in the determination of the distribution of biological species and drugs within the living cell.<sup>32-34</sup>

The SERS effect may be observed for three types of metal surface conditions;<sup>1-10</sup> (1) electrodes with SERS-active surfaces prepared by a specific oxidation-reduction cycle (ORC) occurred in the electrochemical cell. (2) SERS-active metal surfaces having regular 'roughnesses'. (3) metal colloid particles which are small in size by comparison with the wavelength of the incident light. Recently, particular attention has been paid to the metal colloid systems because a few groups succeeded in probing single molecules and single nanoparticles on silver colloid by SERS.<sup>35,36</sup> SERS of molecules adsorbed on colloidal silver and gold particles in solution offers new and interesting possibilities as an analytical tool for detecting various types of molecules at extremely low concentrations.

This review paper is concerned with applications of SERS of metal colloid systems to biological quantitative assay. It consists of two parts. The first part deals with our recent studies on the mechanism of SERS from metal colloid systems. Although the applications of SERS to biological trace analysis have been investigated extensively for the last decade, knowledge about the factors which dominate the sensitivity, stability, and reproducibility of SERS is still not sufficient. It is also not easy to control the experimental conditions of SERS such as the conditions of aggregation of metal colloid.<sup>37-40</sup> Thus, we have undertaken systematic investigations of SERS of simple biological molecules on gold and silver colloid sol to investigate the

interaction between adsorbed molecules and colloidal particles, the mechanism of colloidal aggregation, and structure of adsorbed molecules which may determine the sensitivity, stability, and reproducibility of SERS.<sup>20,21</sup>

In the second part of this review our recent studies on applications of SERS to trace assays of biological molecules are described. We have been exploring bioanalytical applications of SERS.<sup>27,30,31</sup> For example, we reported a new enzyme immunoassay based on SERS which has detection limit of  $\sim 10^{-15}$  mol/ml<sup>30</sup> and quantitative analysis of double-stranded DNA amplified by a polymerase chain reaction employing SERS.<sup>27</sup> Silver colloidal sol were utilized for both cases.

## 2. MECHANISM OF SURFACE-ENHANCED RAMAN SCATTERING OF SIMPLE BIOLOGICAL MOLECULES ON METAL COLLOID

This chapter reports the investigations of the mechanism of SERS of amino acids on gold colloid. The first part presents the effects of electrostatic interaction between adsorbed molecules and gold colloid and of steric hindrance of the molecules on the intensity of SERS. The second part deals with effects of aggregation of gold colloid on SERS of biological molecules.

### 2.1 Effects of pH of the Solutions of Amino Acids and Their Polymerization on Surface-Enhanced Raman Scattering of Simple Biological Molecules on Gold Colloid

In this study amino acids were employed to explore the mechanism of SERS on metal colloid. Amino acids are superior materials for the investigations of the electrostatic interaction between the adsorbed molecules and the metal colloid because they are ampholyte; both carboxyl and amino groups are ionized in the amino acids. The electrostatic states of amino acids change with pH, so that the interaction between the amino acids and gold colloid, which has negative potential, also changes with pH. Each amino acid has  $pK_1$  and  $pK_2$ ; for Lys, they are 2.16 and 9.18, respectively, and they are 2.35 and 9.78, respectively, for Gly. The isoelectric point  $pI$  of the amino acids can be defined as follows;

$$pI = 1/2 (pK_1 + pK_2) \quad (1)$$

Another advantage of amino acids for the studies of SERS mechanism is the ability of the formation of oligomers and polymers; one can investigate the effects of polymerization on the SERS intensity by use of amino acids.

In order to investigate the effects of pH and polymerization on the SERS spectra of Lys and Gly, we employed gold colloid because it is more stable than silver colloid and chemical contribution to SERS is much less for gold colloid.<sup>20</sup> For the gold colloid system the near-infrared excitation was used because it is more effective for the emergence of SERS.<sup>41,42</sup>

Figure 1 (A) and (B) shows the 802 nm-excited SERS spectra of Lys adsorbed on gold colloid in the solutions of pH 10.8 and 12.0, respectively.<sup>20</sup> Interestingly, SERS intensity increases dramatically upon going from pH 12.0 to pH 10.8. The pK of  $\epsilon$ -amino group of Lys is 10.8, and thus at pH 10.8 some of the  $\epsilon$ -amino groups have positive charge and most of the carboxyl groups have negative charge. At pH 12.0 both the  $\alpha$ - and  $\epsilon$ -amino groups are in neutral states, so that Lys assumes the anion form. The pH-dependent changes in the SERS intensity in Figure 1 suggest that the electrostatic interaction between the positive charge of  $\text{NH}_3^+$  group and negative charge on gold colloid plays an important role in the emergence of SERS effect.<sup>20</sup> Figure 2 illustrates the structure of Lys and the mechanism of its adsorption on gold colloid.

Figure 3 (A), (B), and (C) depicts Raman spectra of Lys solutions (20 wt%) at pH 6.0, 10.0, and 12.0, respectively.<sup>20</sup> According to the previous studies of the Raman spectra of amino acids,<sup>43-47</sup> four bands at 1437, 1408, 1348 and 1318  $\text{cm}^{-1}$  may be assigned to  $\text{CH}_2$  bending,  $\text{COO}^-$  symmetric stretching,  $\text{CH}$  bending, and  $\text{CH}_2$  wagging modes, respectively. Bands at 1070, 985, 919, and 854  $\text{cm}^{-1}$  are due to C-N or C-C stretching modes. The band assignments for the SERS and Raman spectra of Lys are summarized in Table 1.<sup>20</sup>

It is of note that the intensities of Raman bands change markedly between the SERS and normal Raman spectra of Lys (Figures 1 and 3). For example, intense bands at 987 and 932  $\text{cm}^{-1}$  in the SERS spectrum are missing or very weak in the Raman spectra. It is very likely that these spectral changes are caused by the electrostatic interaction between the  $\text{NH}_3^+$  group of Lys and the gold colloid. In general,  $\text{NH}_3^+$  groups do not yield an intense band in a Raman spectrum in the 1800-500  $\text{cm}^{-1}$  region, but a band at 1605  $\text{cm}^{-1}$  in Figure 1 (A) may be due to the  $\text{NH}_3^+$  asymmetrical deformation mode.<sup>20</sup> According to the surface selection rule in SERS spectra,<sup>4,12</sup> if Lys adsorbs on the gold surface via its  $\epsilon\text{-NH}_3^+$  group, a band due to the  $\text{C}_\epsilon\text{-N}$  stretching mode

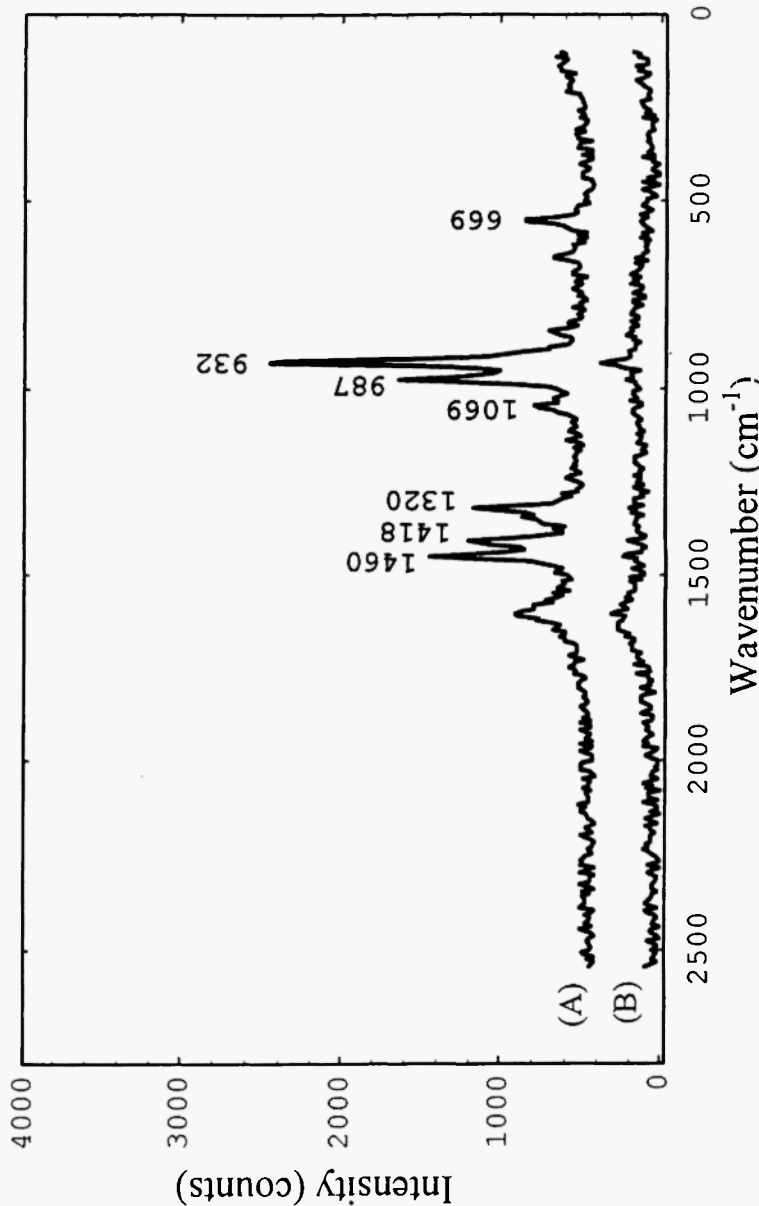
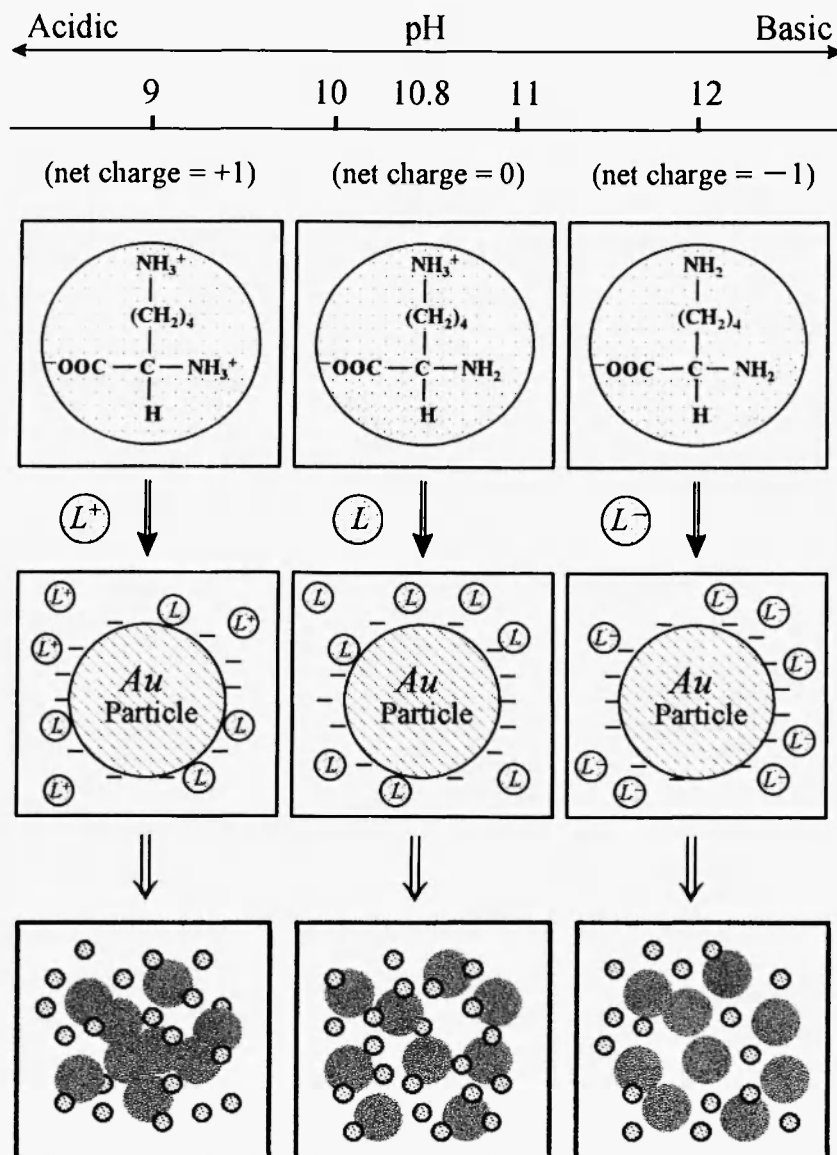


Fig. 1: SERS spectra of Ly s adsorbed on gold colloid in aqueous solutions of pH 10.8 (A) and 12.0 (B). (Reproduced from ref. 20 with permission. Copyright (1999) Society for Applied Spectroscopy)



**Fig. 2:** pH-dependent changes in structure and net charge of L-lysine and the mechanism of its adsorption on gold colloid. (Reproduced from ref. 20 with permission. Copyright (1999) Society for Applied Spectroscopy)

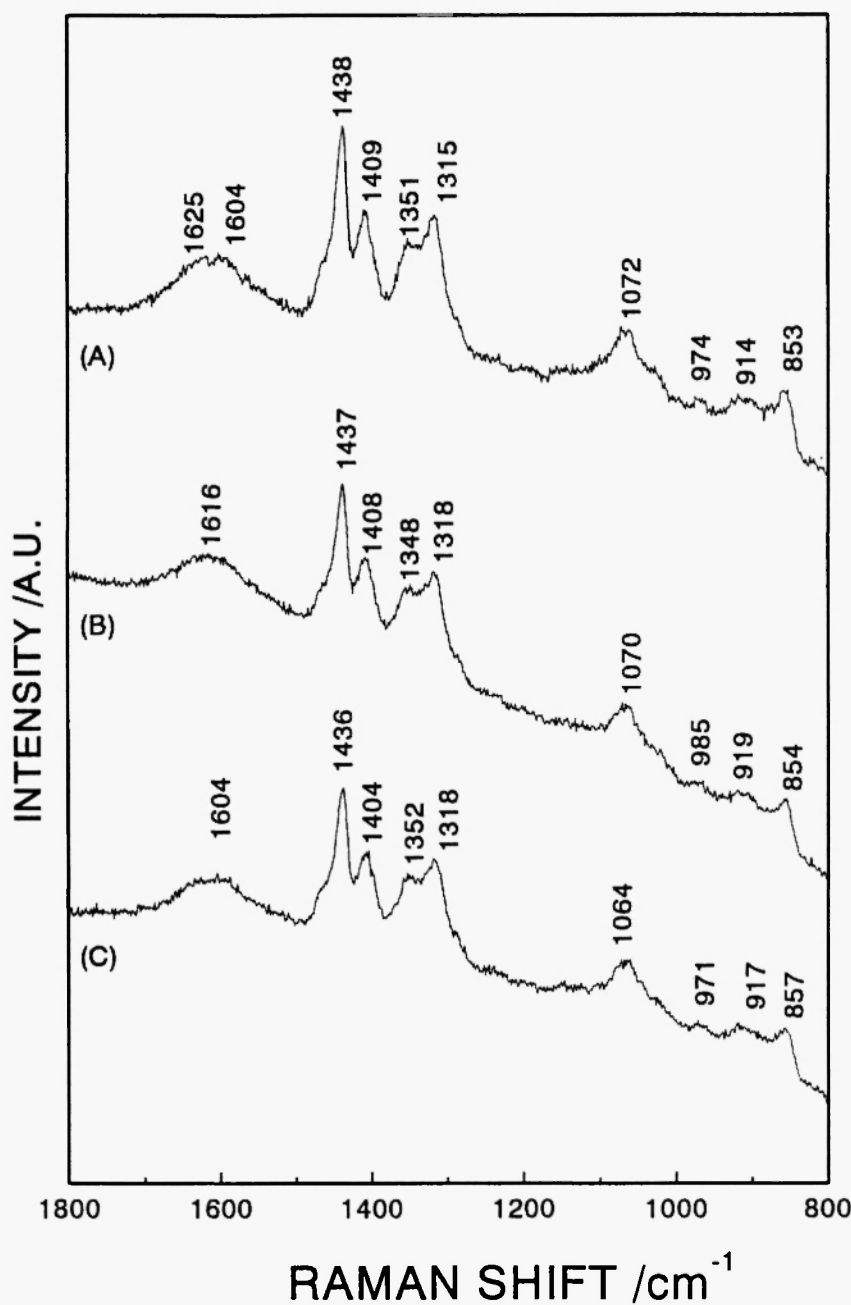


Fig. 3: Raman spectra of Lys in aqueous solutions (20 wt%) at pH 6.0 (A), 10.0 (B), and 12.0 (C). (Reproduced from ref. 20 with permission. Copyright (1999) Society for Applied Spectroscopy)

Table 1

Frequencies (cm<sup>-1</sup>) and assignments of bands in the normal Raman  
and SERS of lysine

Solution (pH 10.0)	SERS for gold colloid	Assignments
1616 (b)	1605 (m) 1460 (m)	NH <sub>3</sub> <sup>+</sup> asym. stret. + water band CH <sub>2</sub> bend.
1437 (s)		CH <sub>2</sub> bend.
1408 (m)	1418 (m)	COO <sup>-</sup> sym. stret.
1348 (m)	1346 (sh)	CH bend.
1318 (m)	1320 (m)	CH <sub>2</sub> wag.
1070 (m)	1069 (w)	C-N stret.
985 (vw)	987 (m) 932 (s)	C-C stret. C-N stret.
919 (w)		C-C stret.
854 (w)	860 (w)	C-C stret.
	654 (w)	COO <sup>-</sup> bend.

Note: b = broad; m = medium; s = strong; sh = shoulder; vw = very weak;  
w = weak.

should appear strongly in the SERS spectrum. Thus, we assigned the intense band at 932 cm<sup>-1</sup> to the C<sub>ε</sub>-N stretching mode.

Although the Raman scattering intensity changes between the SERS and normal Raman spectra of Lys (Figures 1(A) and 3), the frequency shifts are small. Therefore, it may be concluded that the contribution of the chemical mechanism to SERS is small for Lys on the gold colloid.<sup>20</sup>

SERS spectra of Gly on gold colloid are displayed as a function of pH in Figure 4.<sup>20</sup> The SERS intensity decreases markedly above pH 10.0, which is higher than the pK<sub>2</sub> of Gly (9.78). This observation also suggests that the positively charged amino groups interact with negatively charged gold surface, yielding SERS effects.

A Raman spectrum of Gly solution (20 wt%) at pH 6.0 is shown in Figure 5.<sup>20</sup> Table 2 summarizes the band assignments for the SERS and Raman spectra of Gly solutions shown in Figures 4 and 5. It can be seen from comparison between Figures 4 and 5 that again, there are marked spectral

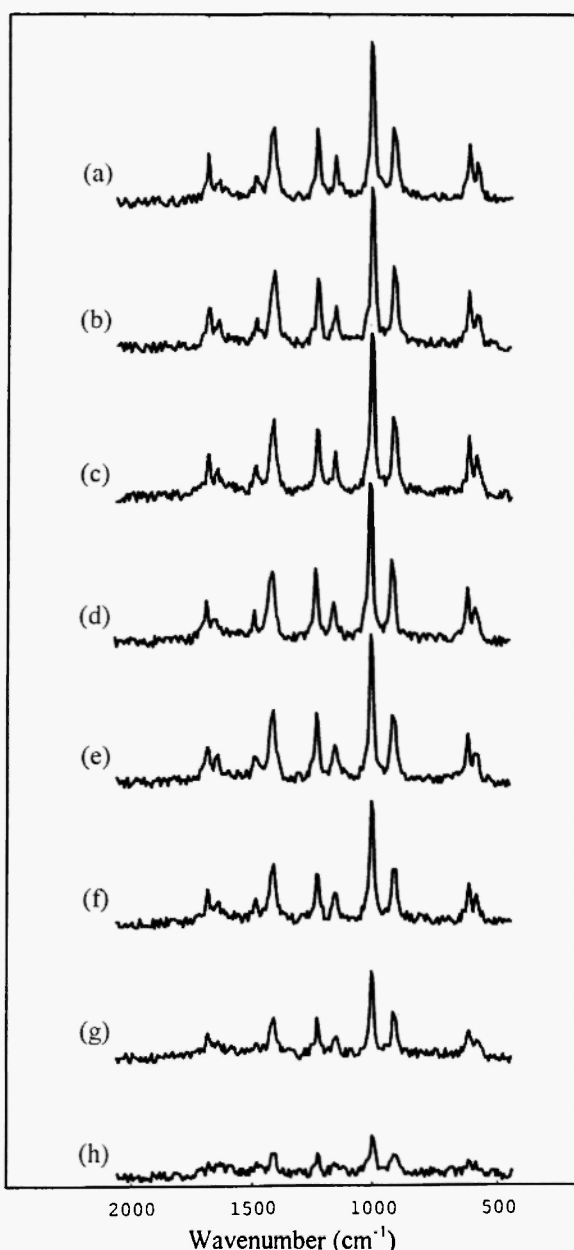


**Fig. 4:** SERS spectra of Gly adsorbed on gold colloid in aqueous solutions of various pH. (a) pH 2.0; (b) pH 4.2; (c) pH 5.5; (d) pH 6.6; (e) pH 7.5; (f) pH 8.2; (g) pH 10.0; (h) pH 12.0. (Reproduced from ref. 20 with permission. Copyright (1999) Society for Applied Spectroscopy)

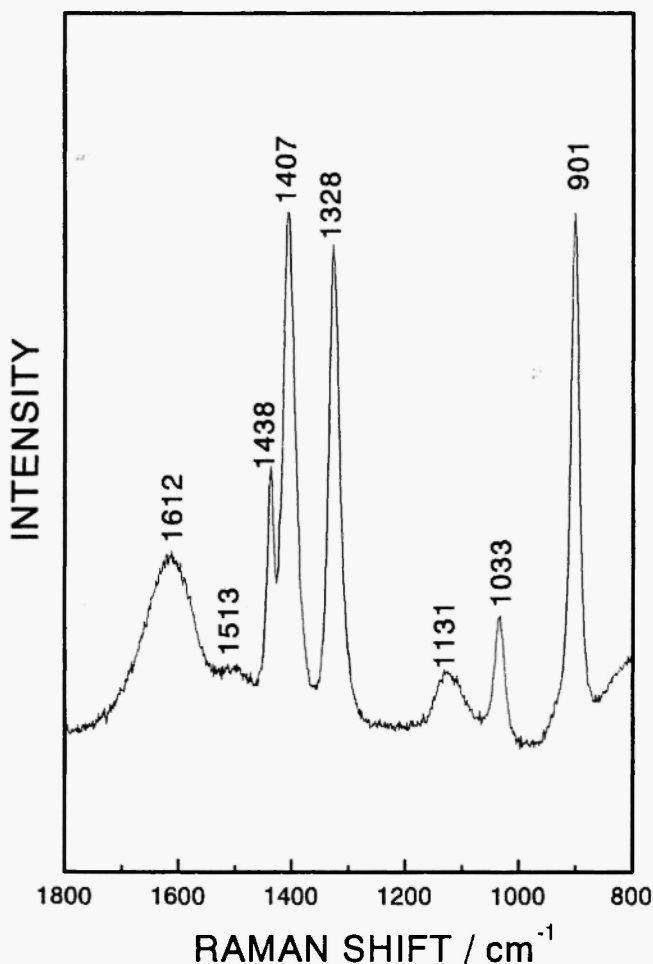


**Fig. 5:** A Raman spectrum of Gly in an aqueous solution (20 wt%) at pH 6.0. (Reproduced from ref. 20 with permission. Copyright (1999) Society for Applied Spectroscopy)

changes between the SERS and Raman spectra. A notable example in the changes is that the SERS spectrum shows an intense band at  $1003 \text{ cm}^{-1}$  and a medium band at  $1234 \text{ cm}^{-1}$ , but the corresponding bands are not identified in the Raman spectrum. It is noted that a band at  $1405 \text{ cm}^{-1}$  due to the  $\text{COO}^-$  symmetric stretching band does not shift upon the adsorption on the gold colloid probably because the  $\text{COO}^-$  group does not interact directly with the

**Table 2**  
 Frequencies ( $\text{cm}^{-1}$ ) and assignments of bands in the normal Raman  
 and SERS of glycine

Solution (pH 6.0)	SERS for gold colloid	SERS for silver colloid	Assignments
	1672 (m)		$\text{COO}^-$ asym. stret.
	1656 (w)		$\text{NH}_3^+$ asym. def.
1612 (br)		1608 (w)	$\text{NH}_3^+$ asym. def.
		1542 (w)	
1513 (vw)	1490 (w)		$\text{NH}_3^+$ sym. def.
1438 (m)			$\text{CH}_2$ bend.
1407 (vs)	1405 (m)		$\text{COO}^-$ sym. stret.
		1383 (vs)	$\text{COO}^-$ sym. stret.
1328 (vs)			$\text{CH}_2$ wag.
	1234 (m)	1226 (vw)	
	1150 (m)		
1131 (w)		1122 (m)	$\text{NH}_3^+$ rock.
1033 (m)		1032 (s)	C-N stret.
	1003 (s)		C-N stret.
	920 (m)	912 (m)	C-C stret.
901 (vs)			C-C stret.
	607 (m)		$\text{COO}^-$ wag.

Note: b = broad, m = medium; s = strong; vw = very weak; vs = very strong; w = weak.

gold colloid. Strong evidences for the electrostatic interaction between the  $\text{NH}_3^+$  group and the gold surface come from the enhancement of the  $\text{NH}_3^+$  asymmetric and symmetric stretching modes at 1656 and 1490  $\text{cm}^{-1}$ , respectively, and of the C-N stretching mode at 1003  $\text{cm}^{-1}$ .<sup>20</sup>

Figure 6 shows a SERS spectrum of Gly solution on aqueous silver sol reported by Suh and Moskovits.<sup>12</sup> Note that the spectrum is quite different from the SERS spectrum of the Gly solution on gold colloid. The  $\text{COO}^-$  symmetric stretching band appears at 1383  $\text{cm}^{-1}$  in the SERS spectrum of Gly on the silver colloid.<sup>12</sup> It seems very likely that the  $\text{COO}^-$  group is involved in the interaction between Gly and the silver colloid.<sup>12</sup> Another interesting point in the SERS spectrum in Figure 6 is a band at 241  $\text{cm}^{-1}$  due to a Ag-N ( $\text{NH}_2$  group) stretching mode.<sup>12</sup> Therefore, the effects of chemisorption are very

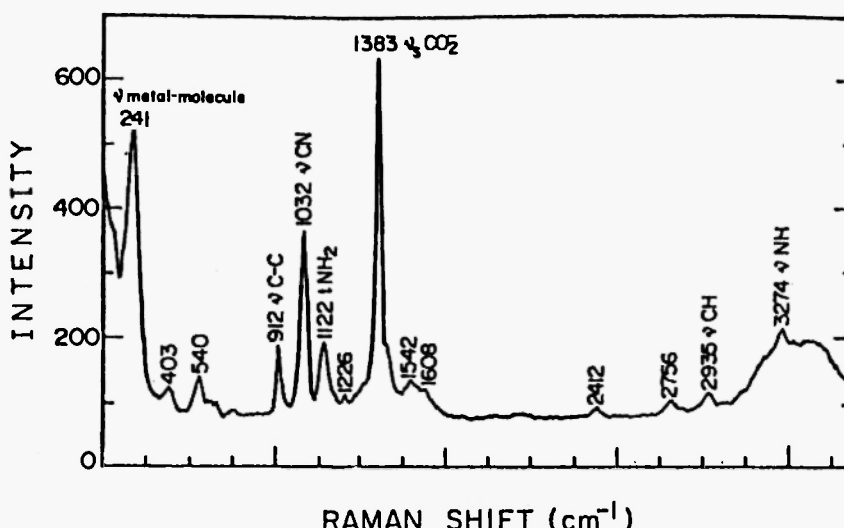


**Fig. 6:** A SERS spectrum of Gly absorbed on silver colloid in an aqueous solution. (Reproduced from ref. 12 with permission. Copyright (1986) American Chemical Society)

important for the amino acid and silver colloid system. The nature of the adsorption of amino acids on the metal colloid and the mechanism of SERS are largely different between the gold and silver colloid. For the gold colloid system, frequency shifts of Raman bands are relatively small, and a band assignable to an Au-amino acid stretching mode is not observed. It has been generally considered that the chemical mechanism does not play a key role in the emergence of SERS effect for the gold colloid system.

Figure 7 displays SERS spectra of Lys, its oligomers and polymers on gold colloid.<sup>20</sup> The degree of polymerization (n) is 1(A), 3(B), 5(C), 17(D), 65(E), and 154(F), respectively. The SERS intensity is reduced markedly with the increase in the degree of polymerization. The SERS intensity at 932  $\text{cm}^{-1}$  vs. the molecular weight of oligomers and polymers of Lys is plotted in Figure 8.<sup>20</sup> Figure 8 reveals that the enhancement factor of SERS depends crucially upon the molecular weight. SERS spectra of Gly, its oligomers and polymers on gold colloid were also measured, and the similar effect of the polymerization on the SERS intensity was observed.<sup>20</sup>

The marked decrease in the SERS intensity with the polymerization was explained by two factors. One is the steric hindrance of the peptide

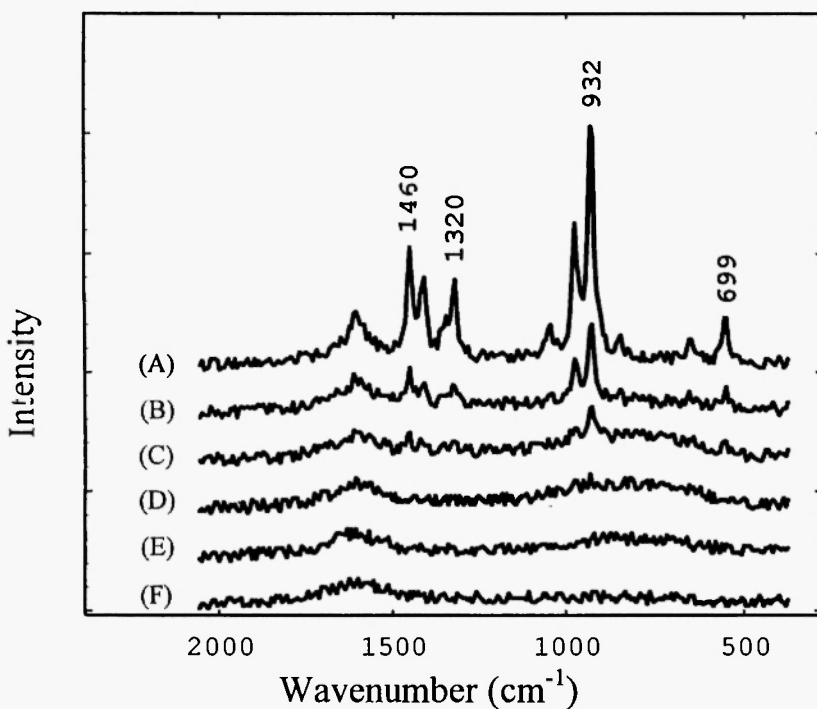


**Fig. 7:** SERS spectra of Lys and its oligomers and polymers adsorbed on gold colloid. Degree of polymerization; (A)  $n=1$ , (B)  $n=3$ , (C)  $n=5$ , (D)  $n=17$ , (E)  $n=65$ , (F)  $n=154$ . (Reproduced from ref. 20 with permission. Copyright (1999) Society for Applied Spectroscopy)

backbones. Because of the steric hindrance, the polymeric species can not adsorb easily on the surface of gold colloid; the population of Lys molecules occupying the metal surface is much less for the polymeric species than for the monomeric species. Another important factor is the average distance between the amino acid unit and the metal surface. This distance is longer for the larger polymers, resulting in the reduction of the SERS effect.

## 2.2 Effects of Aggregation of Gold Colloid on Surface-Enhanced Raman Scattering of Simple Biological Molecules

In order to investigate further the mechanism of SERS on metal colloid system, we studied the relation between the SERS intensity and the

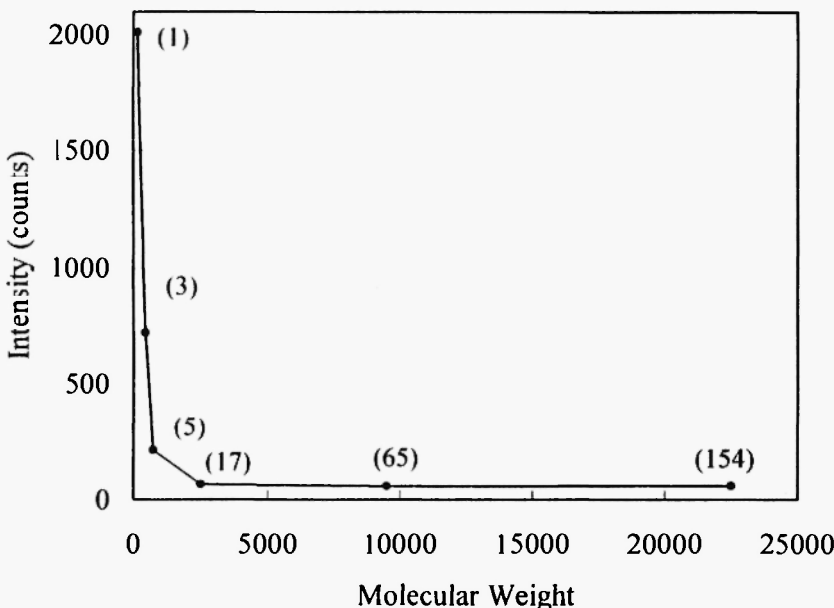


**Fig. 8:** Plots of the SERS intensity at  $932\text{ cm}^{-1}$  of Lys versus its molecular weight. (Reproduced from ref. 20 with permission. Copyright (1999) Society for Applied Spectroscopy)

aggregation of gold colloid particles for Gly in aqueous solutions.<sup>21</sup> For this purpose we developed a Raman scattering-surface plasmon absorption simultaneous measurement system which enables one to measure time-dependent SERS and an absorption intensity change at 802 nm of Gly on the gold colloid at the same time. Figure 9 illustrates the system that we developed.<sup>21</sup> The colloid is activated by electrolyte-induced aggregation, and the aggregation process can be monitored by the broad absorption in the 760-810 nm region due to surface plasmon.<sup>38</sup> Therefore, it is very important to measure the SERS and absorption intensity simultaneously.

Figures 10 (a), (b), and (c) show UV-Vis spectra of Gly on the gold colloid at pH 9.8, 6.0, and 3.9.<sup>21</sup> The spectra shown in Figure 10 were obtained 30 seconds after the mixing of the Gly solution with the colloid solution. The spectrum at pH 9.8 is very close to a typical spectrum of gold colloid sol with a diameter of 30 nm. Since both the gold colloid and Gly have negative charge at pH 9.8, Gly molecules do not adsorb on the colloid

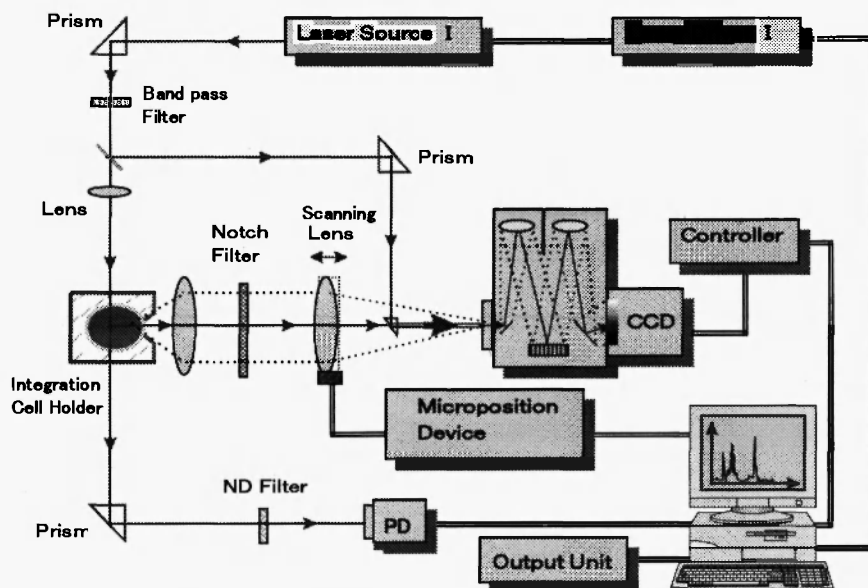


**Fig. 9:** A Raman scattering-surface plasmon absorption simultaneous measurement system. (Reproduced from ref. 21 with permission. Copyright (1999) Society for Applied Spectroscopy)

surface. The other two spectra in Figure 10 show a broad band in the 760-790 nm region. This suggests that the aggregation of gold colloid is induced in the neutral and acidic solutions by the electrostatic interaction between the positive charge of the  $\text{NH}_3^+$  group and the negative charge on the gold colloid surface. The appearance of the broad feature in the 760-810 nm region is a good indicator for the aggregation.

The gold colloid particles have negative  $\zeta$  potential and thus are stabilized by electric repulsive force. It is very unlikely that such gold particles form aggregates unless some additives are added to them. If negatively charged molecules, for example, Gly molecules in an aqueous solution of pH 9.8 are mixed with the gold colloid solution, very little interaction is expected to occur between the gold colloid and Gly molecules because both have negative charge. On the other hand, if molecules with the positive charge, for example, Gly molecules in an aqueous solution of pH 6.0 or 3.9 are added to the gold colloid, irreversible aggregation occurs due to the electrostatic interaction between the negative charge of gold colloid and the positive charge of Gly molecules.

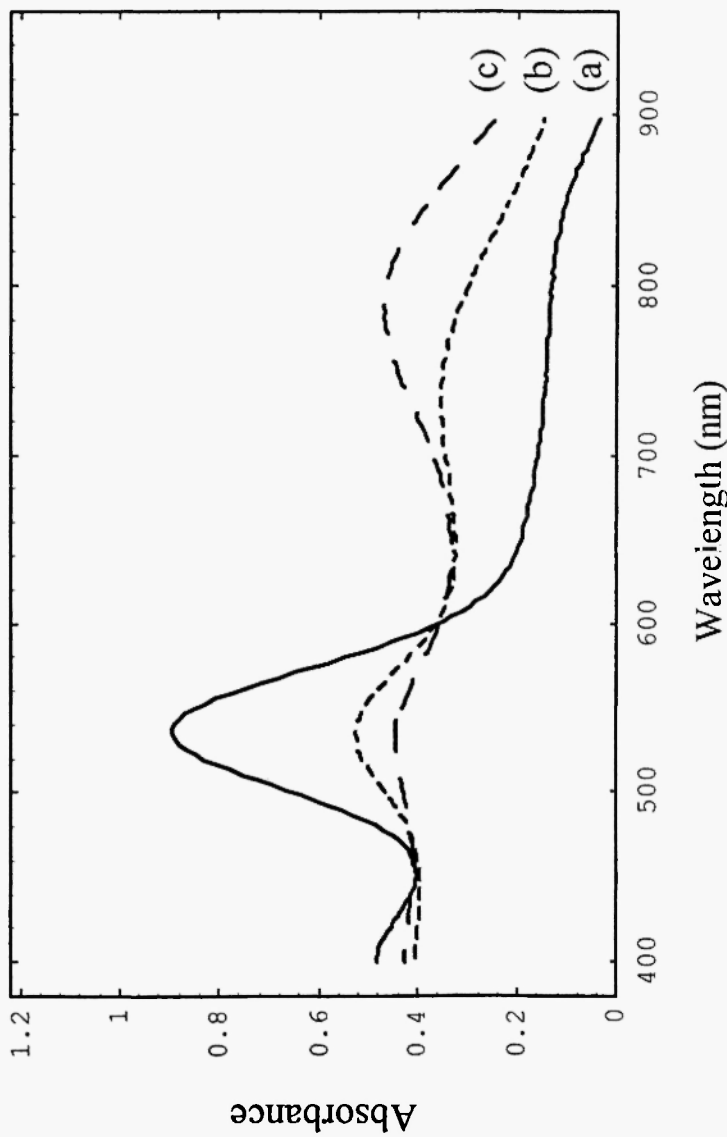


**Fig. 10:** UV-Vis spectra of Gly adsorbed on gold colloid in aqueous solutions of pH 9.8 (a), 6.0 (b), and 3.9 (c). (Reproduced from ref. 21 with permission. Copyright (1999) Society for Applied Spectroscopy)

Figures 11 (a) and (b) show time-dependent changes in SERS spectra of Gly adsorbed on gold colloid in aqueous solutions of pH 6.0 and 3.9, respectively.<sup>21</sup> The spectra were obtained every one second after the adding of the Gly solution to the colloidal solutions. Figure 11 (a) reveals that the

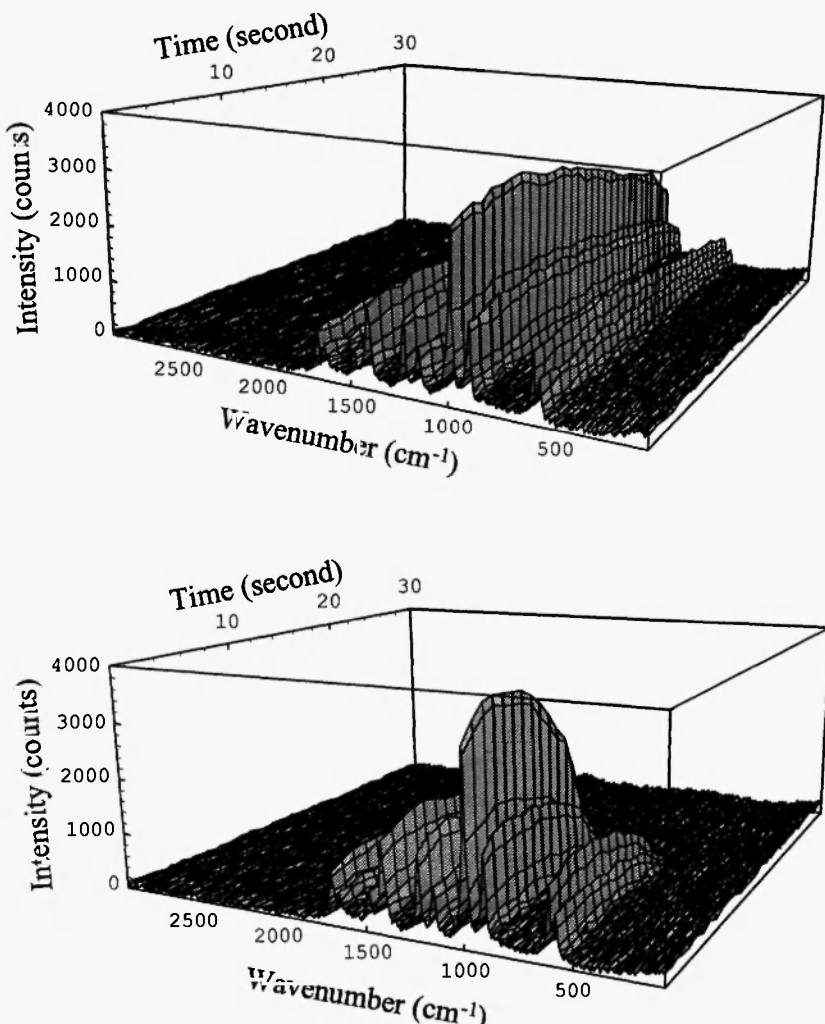


**Fig. 11:** Time-resolved SERS spectra of Gly adsorbed on gold colloid (a; pH 6.0, b; pH 3.9). (Reproduced from ref. 21 with permission. Copyright (1999) Society for Applied Spectroscopy)

SERS intensity increases for a while (about 6 seconds) just after the mixing and then decreases gradually at pH 6.0. It seems that slow coagulation of the gold colloid particles proceeds at pH 6.0 which is close to the isoelectric point of Gly. On the other hand, the SERS intensity changes fast at pH 3.9 (Figure 11(b)). The intensity of the band at  $1003\text{ cm}^{-1}$  due to the C-N stretching mode reaches its maximum about 4 second after the mixing, indicating that the rapid coagulation occurs at pH 3.9. The observation in Figure 11 (b) suggests that if the coagulation proceeds too much, the SERS effect disappears. The time at which the maximum SERS intensity is observed depends upon pH. The period when the SERS is observed also changes with pH. It was concluded that one can observe strong SERS effect for a longer time if one prepares the solution around pH 7.0.<sup>21</sup>

Figure 12 shows a time-dependent change in the absorbance in 802 nm.<sup>21</sup> It is noted that the time-dependent change in the SERS intensity is in parallel with that in the absorbance at 802 nm until about 8 second after the mixing (Figure 11(b) and 12). Therefore, it may be concluded that the emergence of the SERS effect is strongly related to coagulation of gold colloidal particles. The SERS intensity becomes weak rapidly (Figure 11(b)), but the absorbance remains almost unchanged, indicating that the coagulation proceeds too much about 10 second after the mixing.<sup>21</sup>

### 3. APPLICATIONS OF SERS OF METAL COLLOID SYSTEM TO BIOLOGICAL QUANTITATIVE ASSAY

As already described in the Introduction, a large amount of literature is available for biological quantitative assay by SERS.<sup>22-31</sup> In this review we discuss three examples of biological quantitative assay by SERS selected from our recent studies.<sup>27,30,31</sup> Two of them are concerned with "indirect SERS method" which indirectly analyzes the object by observing SERS spectra of another compound.<sup>27,30</sup> By use of the idea of indirect SERS method, we increased markedly the sensitivity of SERS in enzyme immunoassay (see 3.2).<sup>30</sup> In another case (see 3.1), the indirect SERS method has enabled us to carry out quantitative analysis of double-stranded (ds)-DNA.<sup>27</sup>

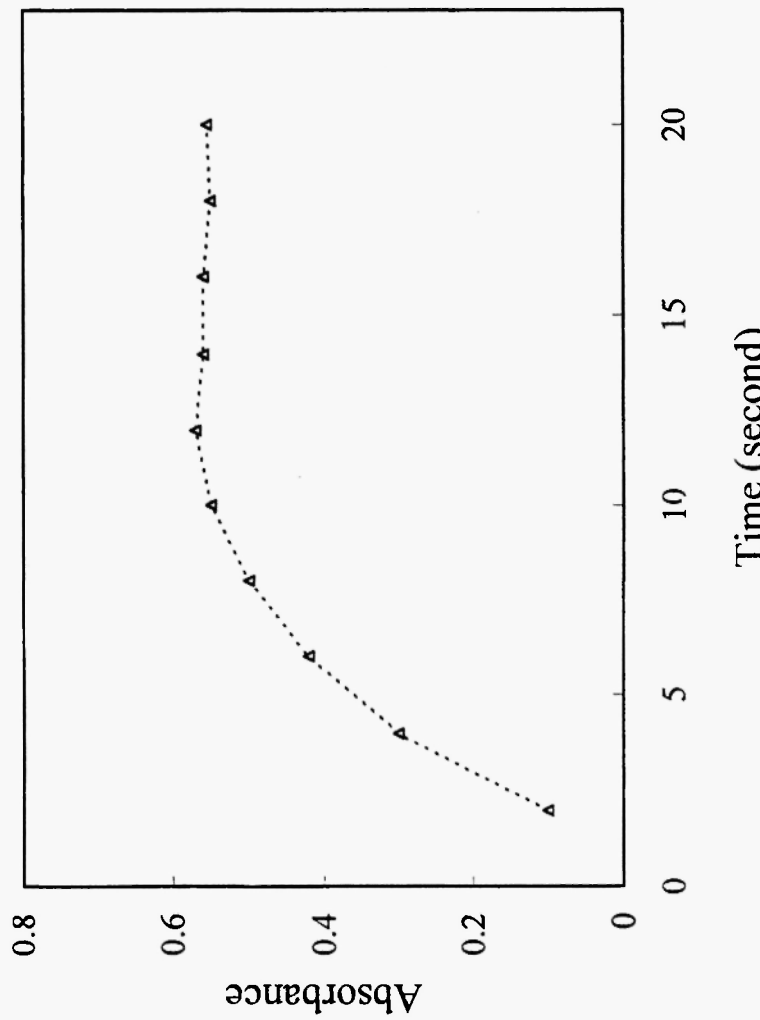


**Fig. 12:** Time-resolved absorption intensity change at 802 nm of Gly adsorbed on gold colloid at pH 3.9. (Reproduced from ref. 21 with permission. Copyright (1999) Society for Applied Spectroscopy)

### 3.1 Quantitative Analysis of Double-stranded DNA Amplified by Polymerase Chain Reaction by Indirect Surface-Enhanced Raman Scattering Method

The examination of the amplification by polymerase chain reaction (PCR) is usually carried out by agarose gel electrophoresis.<sup>48,49</sup> It is time and reagent consuming technique, and requires a control of buffer and gel concentrations depending upon the length of ds-DNA amplified. Therefore, development of simpler and more rapid technique for the examination of the DNA amplification has long been desired. Recently, Vo-Dinh *et al.*<sup>26</sup> proposed DNA gene probes utilizing SERS. Their method uses Cresyl Fast Violet as a label for a specific nucleotide sequence.<sup>26</sup> This probe, which binds to its complementary nucleotide sequence in the DNA fragments investigated, shows intense SERS signals, enabling to detect ds-DNA. However, the process is rather complicated,<sup>26</sup> it requires the labeling of the dye, the separation of the free and bound dyes, and the silver-evaporation on alumina.

We have proposed a simple SERS based method for quantitative analysis of ds-DNA amplified by PCR.<sup>27</sup> We adopted the method which can determine the concentration of ds-DNA indirectly because, in general, ds-DNA does not show an intense SERS signal. Figure 13 illustrates the principle of our method for the quantitative analysis of ds-DNA.<sup>27</sup> In our method, the concentration of ds-DNA is indirectly estimated by measuring the concentration of the dye which does not form a complex with ds-DNA but remains in a solution. As a DNA intercalation material, 4',6-diamidino-2-phenylindole dihydrochloride (DAPI; Figure 13 (D)) was used. DAPI is, so-called, a deeply intercalating dye, and thus DAPI-ds-DNA complexes do not show significant SERS signal. In contrast, free DAPI on the silver colloid emerges very intense SERS signals. If the amount of ds-DNA is small compared with that of DAPI, a large amount of DAPI remains as free DAPI in a solution (Figure 13 (B), the right-hand side). Thus, the strong SERS signals can be obtained (Figure 13 (C), the right-hand side). On the other hand, if there is a large amount of ds-DNA in the solution (Figure 13 (B), the left-hand side), most of the DAPI molecules are intercalated inside the DNA double helix, giving no SERS signal (Figure 13 (C), the left-hand side). Therefore, the concentration of ds-DNA is inversely proportional to the intensity of SERS signals of free DAPI. In this way, one can estimate it indirectly from the intensity of SERS signals from free DAPI.<sup>27</sup>

The DNA intercalation materials can be classified into two groups; deeply intercalating chromophores and not-deeply intercalating ones. DAPI and

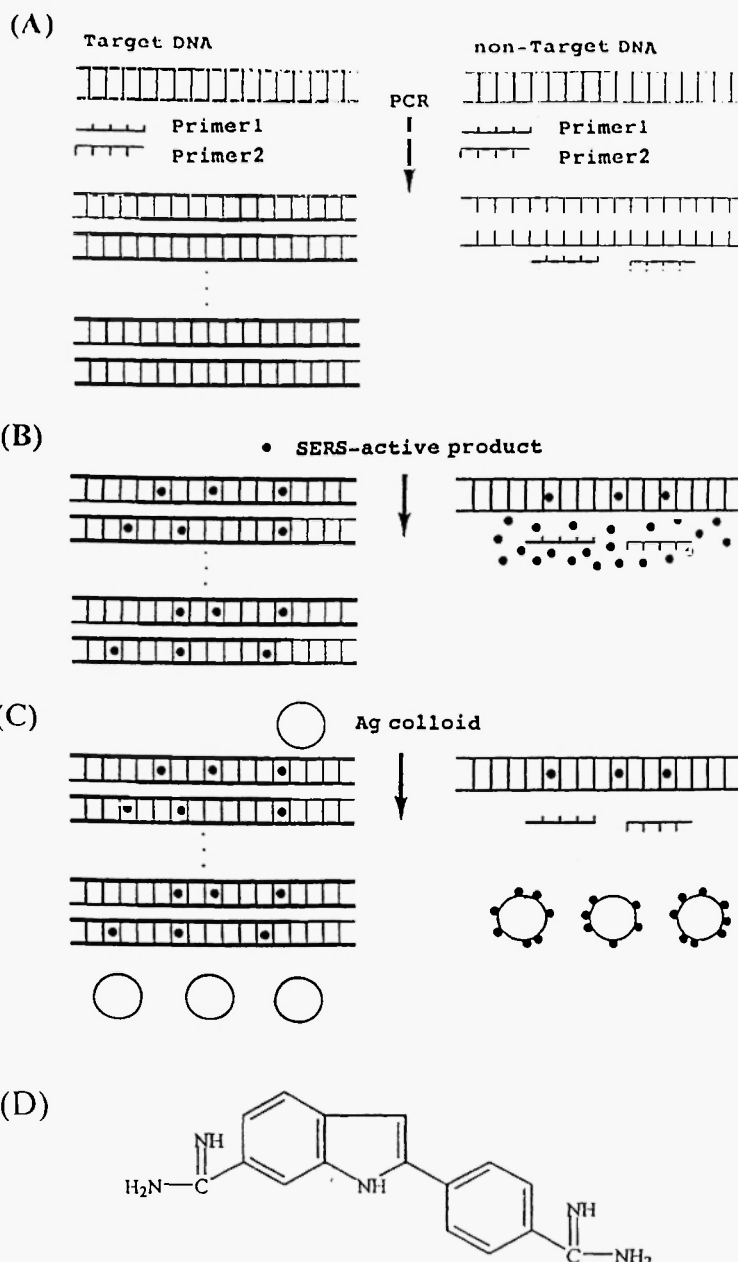


**Fig. 13:** (A) – (C) Principle for quantitative analysis of ds – DNA amplified by PCR utilizing SERS. (D) 4',6 – diamidino-2-phenylindole dihydrochloride (DAPI).

aclacinomycin are examples of the deeply intercalating dyes. The SERS intensities of their complexes with DNA are negligible compared with those of free dyes.<sup>8,50</sup> This phenomenon has been explained in terms of the short-range character of SERS effect in metal colloid systems.<sup>8,50</sup> In contrast to the deeply intercalating chromophores, chromophores of some dyes are not deeply buried in the ds-helix. Saintopin is an example of this group.<sup>51</sup>

Figure 14 shows a Raman spectrum of  $10^{-4}$  M DAPI in an aqueous solution after the addition of a 360  $\mu$ l solution of silver colloid.<sup>27</sup> A number of intense signals are seen in the spectrum. It is the SERS spectrum of DAPI. An intense band at  $1610\text{ cm}^{-1}$  assigned to the C=N stretching mode can be used for estimating the concentration of DAPI.

Figure 15 (a) and (b) compare SERS spectra of the mixture of the PCR, DAPI, and silver colloid solutions for the negative control (35  $\mu$ l of  $10^{-4}$  M DAPI, 5  $\mu$ l of negative PCR solution, and 360  $\mu$ l of a silver colloid solution) and positive control (35  $\mu$ l of  $10^{-4}$  M DAPI, 5  $\mu$ l of positive PCR solution, and 360  $\mu$ l of silver colloid solution) samples, respectively.<sup>27</sup> The SERS spectrum of the NC sample is very similar to the spectrum of DAPI on the silver colloid (Figure 14 (b)) while the SERS signals of the PC sample are very weak or almost missing. The observation in Figure 15 (b) suggests that in the PC sample almost all DAPI molecules are involved in the intercalation with ds-DNA and that there is very little free DAPI.

Figure 16 exhibits dependence of the SERS intensity from the mixture of the PC PCR, DAPI, and silver colloid solutions on the concentration of ds-DNA.<sup>27</sup> Note that the higher the concentration of ds-DNA, the weaker the SERS signals. The results in Figure 16 shows that the concentration of ds-DNA can be determined indirectly by the intensity of the SERS band at  $1610\text{ cm}^{-1}$  of DAPI adsorbed on the silver colloid.<sup>27</sup>

The intensity of the band at  $1610\text{ cm}^{-1}$  versus the concentration of ds-DNA amplified by PCR was plotted. The correlation coefficient (R) was calculated to be 0.988 for the concentration range from 0.1 to 1.3  $\mu$ l/ml.<sup>27</sup> The PCR amplified the concentration of restriction enzyme of ds-DNA fragment by about  $10^{10}$  times. Therefore, the detection limit of the present system, which allows the enhancement of another factor of about  $10^5$ , can be estimated to be about 0.13 fg/ml of ds-DNA.<sup>27</sup>

The SERS method described above is simpler than the conventional method utilizing agarose gel electrophoresis, is simpler than and can be applied to ds-DNA amplified of any length without changing experimental conditions. It can monitor the conditions of PCR, enabling one to decrease the number of the cycling.

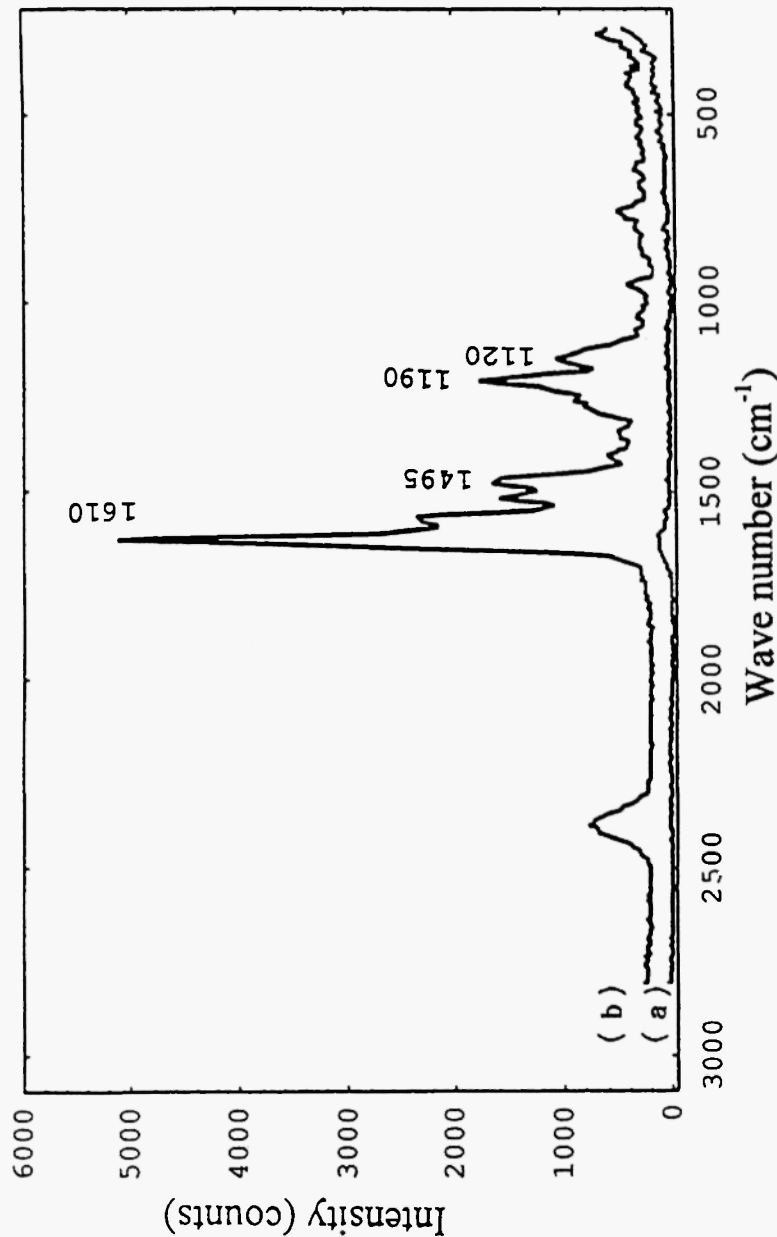
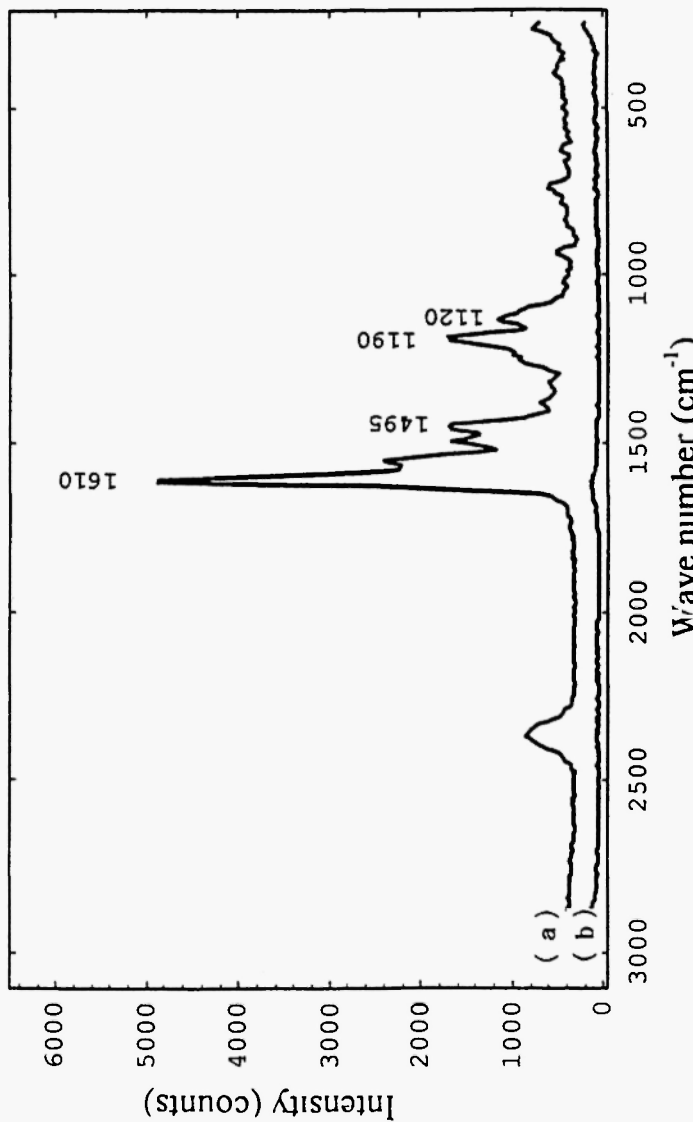
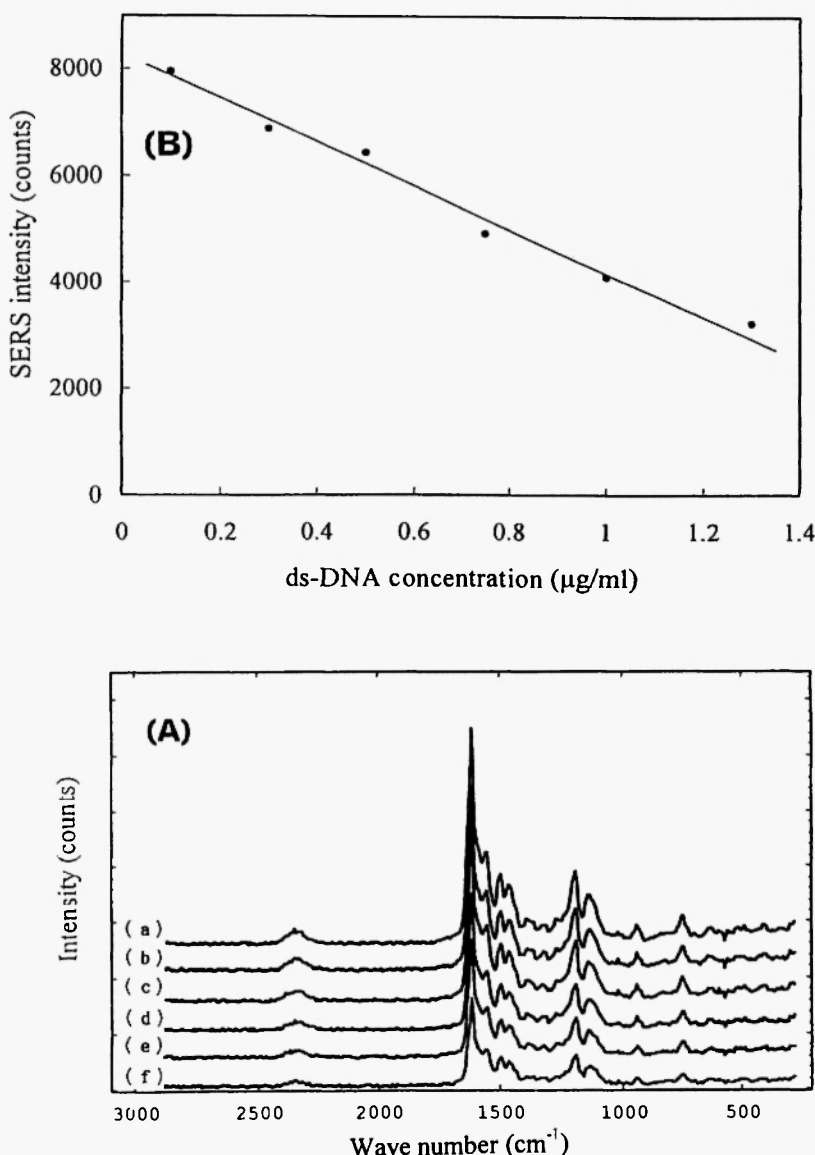


Fig. 14: A Raman spectrum of DAPI ( $10^{-4}$  M) on silver colloid. (Reproduced from ref. 27 with permission. Copyright (1998) Optical Society of America.)



**Fig. 15:** SERS spectra of the mixture of the PCR ( $5\mu\text{l}$ ), DAPI ( $35\mu\text{l}$ ), and silver colloid ( $360\mu\text{l}$ ) solutions. (a) negative control ( $10^4\text{M}$  of DAPI and negative PCR solution), (b) positive control ( $10^4\text{M}$  of DAPI and positive PCR solution). (Reproduced from ref. 27 with permission. Copyright (1998) Optical Society of America).



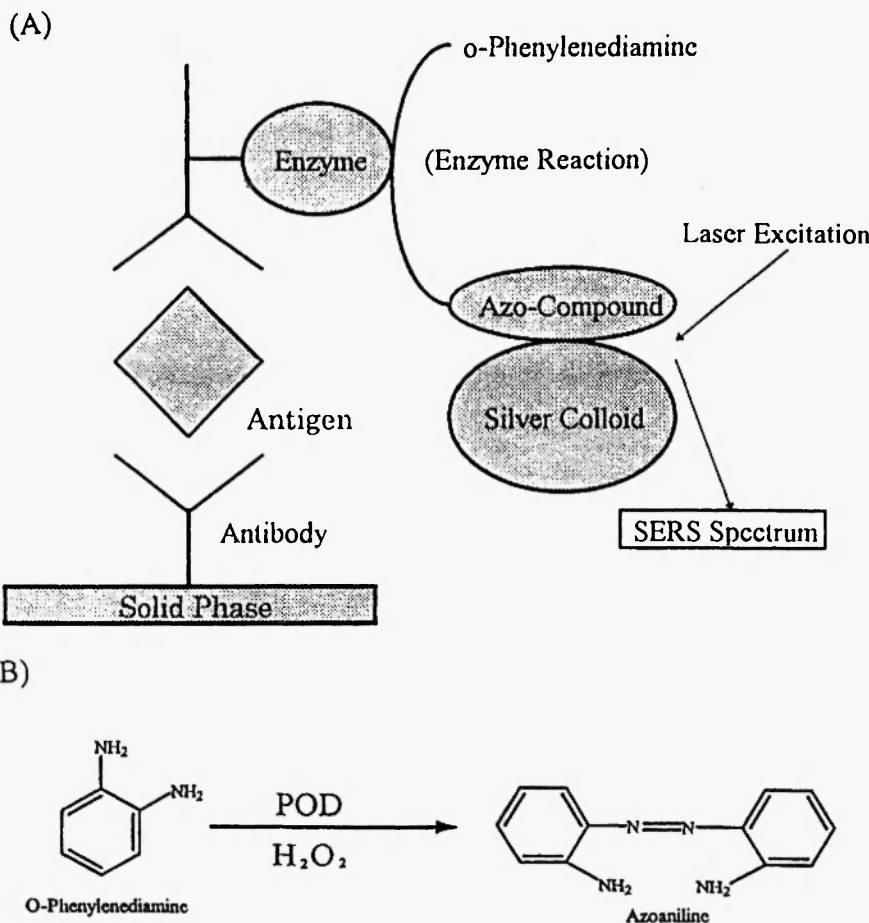
**Fig. 16:** (A) Dependence of the SERS spectrum of the mixture of the PCR (5 µl), DAPI (35 µl), and silver colloid (360 µl) solutions on the concentration of ds-DNA. Concentration: (a) 0.1, (b) 0.3, (c) 0.5, (d) 0.75, (e) 1.0, and (f) 1.3 µl. (B) The SERS intensity at 1610 cm<sup>-1</sup> versus the concentration of ds-DNA amplified by PCR. (Reproduced from ref. 27 with permission. Copyright (1998) Optical Society of America).

### 3.2 Enzyme Immunoassay by Indirect Surface-Enhanced Raman Scattering Method

Raman spectroscopy has been thought to hold considerable promise for enzyme immunoassay because, showing abundant, yet sharp and well-resolved bands, it contains much chemical information useful for enzyme immunoassay.<sup>29-31</sup> However, in general, the sensitivity of Raman spectroscopy is not enough for immunoassay. In order to overcome this difficulty, Cotton *et al.*<sup>29</sup> utilized SERRS effect for Raman enzyme immunoassay. In their system resonance dye, p-dimethylaminoazobenzene (DAB) was attached covalently to an antibody directed against human thyroid stimulating hormone (TSH), and the resultant conjugate was used as the reporter molecule in a sandwich immunoassay for TSH antigen. The intensity of the resultant SERRS signals showed a good correlation with TSH antigen concentration over a range of from 4 to 60 IU/ml.<sup>29</sup>

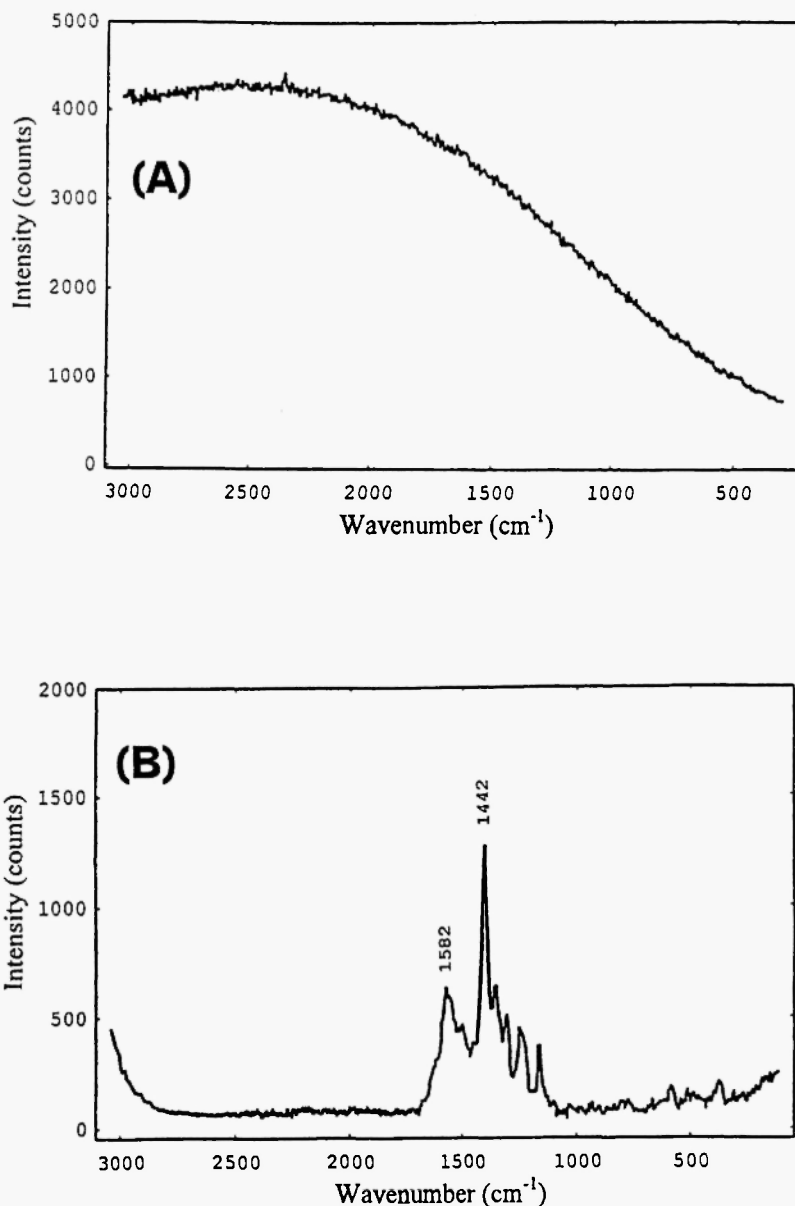
The SERRS method has several advantages for enzyme immunoassay over other spectroscopic techniques. First, the SERRS signal can not overdevelop as in systems based on optical absorbance. Second, unlike fluorescence probe SERRS reporter groups do not self-quench, so that the intensity of the signal can be enhanced by increasing the number of SERRS reporter groups.<sup>29</sup> We have proposed a novel enzyme immunoassay utilizing SERRS method.<sup>30</sup> The detection limit of our system was found to be about  $10^{-15}$  mol/mL, which was lower by one-order than that of the system employed by Cotton *et al.*<sup>29</sup>

Figure 17 illustrates the proposed system.<sup>30</sup> In the system shown in Figure 17, antibody immobilized on a solid substrate reacts with antigen which binds with another antibody labeled with peroxidase (POD). When this immune-complex is reacted with ortho-phenylenediamine and hydrogen peroxide, azoamiline is generated as a reaction product. In order to estimate the concentration of antigen (mouse-IgG), SERRS signals from azoaniline absorbed on silver colloid are measured. The proposed system has several advantages.<sup>30</sup> First, the SERRS reporter group is a simple and stable dye which shows very strong Raman bands due to the N=N and C=C stretching modes. Second, the selectivity is extremely high because only the dye yields SERRS signals. Third, the system determines the concentration of antigen indirectly via the SERS signals of the reaction product. Therefore, the sensitivity of this method is free from the Raman scattering intensity of the label directly attached to antibody. We named this method the indirect SERS method.



**Fig. 17:** (A) Enzyme immunoassay based upon indirect SERS method and (B) enzyme reaction investigated. (Reproduced from ref. 30 with permission. Copyright (1997) American Chemical Society).

Figure 18 (A) shows a normal Raman spectrum of the reaction mixture of  $10^{-6}$  M orthophenylenediamine, 0.1% POD, and 0.136 % hydrogen peroxide after the enzyme reaction. Note that the spectrum shows strong fluorescent background. This is a good example of a serious obstacle for the quantitative analysis of the reaction product by Raman spectroscopy.



**Fig. 18:** (A) A normal Raman spectrum of the reaction product (azoaniline) of the enzyme reaction shown in Figure 17. (B) A SERRS spectrum of the enzyme-substrate mixture after the reaction. (Reproduced from ref. 30 with permission. Copyright (1997) American Chemical Society).

Before we applied the SERRS method to the enzyme reaction mixture, SERS spectra were measured for  $10^{-6}$  M ortho-phenylenediamine, 0.1 % POD, and 0.136 % hydrogen peroxide, independently.<sup>30</sup> No peak was observed in the obtained spectra except for a weak feature around  $1650\text{ cm}^{-1}$  assignable to the bending mode of water. In sharp contrast to these spectra, a SERS spectrum of the reaction mixture of the above three compounds exhibits a number of intense Raman peaks as shown in Figure 18(B).<sup>30</sup> There is little doubt that the SERS signals arise from the enzyme product generated by the oxidation-condensation reaction of ortho-phenylenediamine. Of particular importance is that only the enzyme reaction product yields strong SERS signals and that the enzyme or substrate itself dose not show any detectable SERS peak. In other words, the concentration of the product can be monitored selectively without any interference. It is also noted that the strong fluorescent background is markedly reduced in the SERS spectrum (compare Figure 18 (A) and (B)). Azoaniline on the silver colloid shows an absorption maximum at 420 nm, and the 514.5 nm excitation was used, so that the spectrum obtained may be the SERRS spectrum. Peaks at 1582 and  $1442\text{ cm}^{-1}$  are assigned to the C=C and N=N stretching modes, respectively.

Figure 19 depicts the SERRS spectra of azoaniline produced by the enzyme reaction of ortho-phenylenediamine with peroxide and the immuno-complex labeled by POD.<sup>30</sup> The concentration of the antigen was changed from 0.1575 ng/mL (Figure 19 (d)) to 2.5 ng/mL (Figure 19 (a)). Intensities of the Raman peaks at 1582 and  $1442\text{ cm}^{-1}$  are proportional to the concentration of antigen in the range of 0.375 to 2.5 ng/mL.

A good straight line was obtained between the intensity of the band at  $1442\text{ cm}^{-1}$  versus the concentration of antigen. The correlation coefficient ( $R$ ) between them was calculated to be 0.999 for the concentration range from 0.158 to 2.5 ng/ml.<sup>30</sup> The detection limit of this SERRS enzyme immunoassay method was found to be about  $10^{-15}$  mol/ml, which was lower by 1 order of magnitude than that found for a previously reported method employing SERRS.<sup>30</sup>

The study described above has demonstrated the possibility of enzyme-immunoassay utilizing indirect SERRS method. The sensitivity of this method is not controlled by Raman intensity of reporter molecules covalently bounded with antibody. Therefore, even higher sensitivity might be expected if one could find more proper enzyme reaction system containing immuno-complexes.

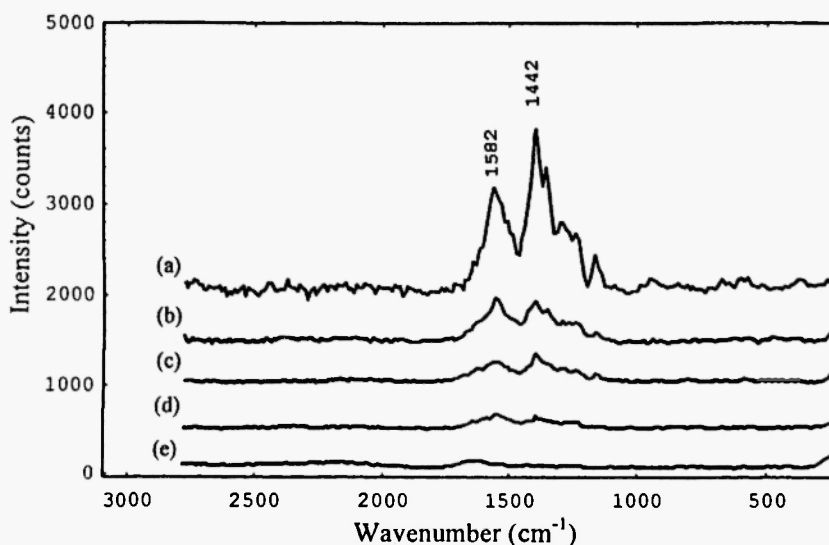


**Fig. 19:** SERRS spectra of the reaction product of ortho-phenylenediamine with the immuno-complex labeled with POD. The concentration of antigen was 2.50 (a), 0.625 (b), 0.315 (c), and 0.1575 (d) ng/mL. The trace (e) is the spectrum of water. (Reproduced from ref. 30 with permission. Copyright (1997) American Chemical Society).

### 3.3 Detection of Immune Reaction without Bound/Free Antigen Separation by Near-infrared Surface-enhanced Raman Scattering

Almost all immunoassays presently employed are so-called heterogeneous immunoassays which need a procedure for the separation of bound and free antigen. However, the B/F separation is a rather cumbersome procedure and reagent consuming. We have demonstrated that near-infrared (NIR) SERS spectroscopy holds considerable promise in detecting the immune reaction on the gold on colloid particles without any procedure for the B/F separation.<sup>31</sup> Figure 20 (a) and (b) illustrates the procedure of our method.<sup>31</sup> Antibody and immune complex are adsorbed on gold colloid particles. Free antigen cannot be adsorbed on the gold colloid surface, since the surface of the gold colloid particles is blocked by bovine serum albumin (BSA). In the system shown in Figure 20, the antibody of  $10^{-8}$  M on the gold colloid particles shows intense SERS signals but the same system of  $10^{-10}$  M

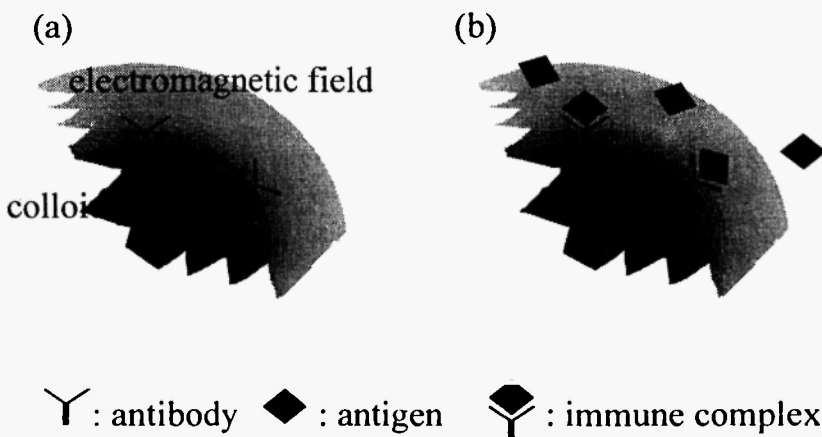


**Fig. 20:** (a) Antibody adsorbed on gold colloid particle. (b) Immune complex on gold colloid particle. (Reproduced from ref. 31 with permission. Copyright (1998) John Wiley & Sons, Ltd.)

does not give any SERS signal. The Raman bands of antibody again appear upon the formation of immunoglobulin (IgG)-anti-IgG complexes on the gold colloid particles.<sup>31</sup>

Figure 21 shows a NIR-SERS spectrum of anti-mouse IgG adsorbed on the gold colloid particles.<sup>31</sup> The spectrum has an appearance fairly different from that of a typical protein Raman spectrum.<sup>52,53</sup> However, bands due to the amide groups (1645 and 1261  $\text{cm}^{-1}$ ) and those assignable to tryptophan (Trp) residues (1467, 1112 and 880  $\text{cm}^{-1}$ ) are clearly identified in the SERS spectrum of Figure 21. Table 3 summarizes the frequencies and assignments of observed Raman bands. It is noted that the bands due to Trp are enhanced largely. Thus far, SERS studies have been carried out for only a few proteins without a prosthetic group.<sup>54-57</sup> According to those studies, bands due to amide I and III are relatively weak in the SERS spectra of proteins, but those due to Trp and tyrosine residues (Tyr) appear strongly. It is also important to point out that the SERS spectra of proteins change markedly with experimental conditions. For example, a SERS spectrum of BSA adsorbed on silver electrode with the potential corresponding to zero charge for silver is different from that of BSA adsorbed on colloidal silver at pH 8.0.<sup>54,56</sup>

The spectrum of Figure 21 provided very interesting information about the adsorption of the protein on the gold colloids.<sup>31</sup> The frequencies of the

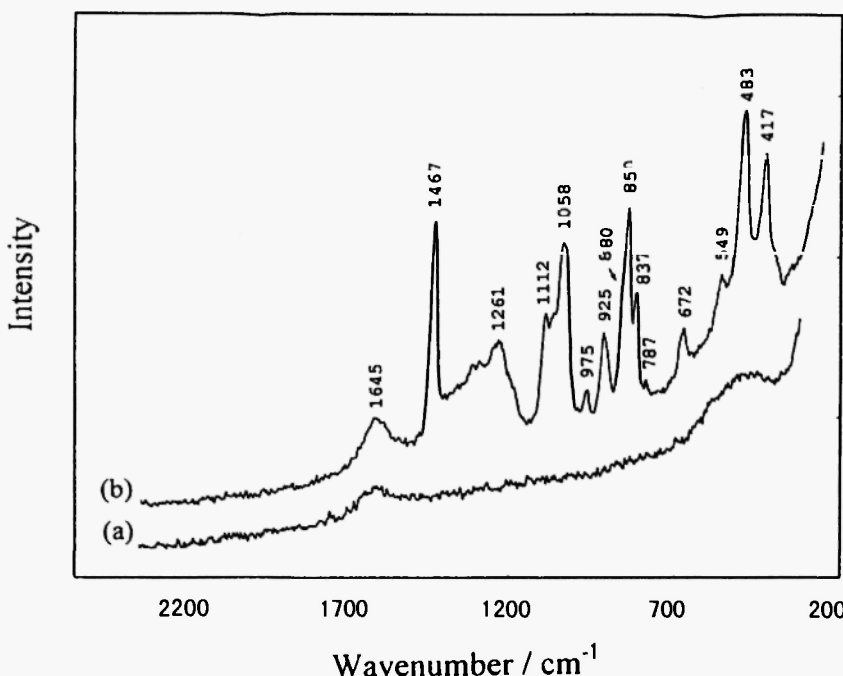


**Fig. 21:** (a) A NIR SERS spectrum of the gold colloid solution. (b) A NIR SERS spectrum of anti-mouse IgG of  $2.2 \times 10^{-8}$  M adsorbed on gold colloid particles. (Reproduced from ref. 31 with permission. Copyright (1998) John Wiley & Sons, Ltd.)

amide I and III bands ( $1645$  and  $1261\text{ cm}^{-1}$ ) are typical of  $\alpha$ -helix structure of a protein.<sup>52,53</sup> However, it is well known that IgG has sheet-rich structure, and, in fact, their amide I and III bands were observed at  $1673$  and  $1239\text{ cm}^{-1}$  in the normal Raman spectra.<sup>58,59</sup> Therefore, the observation in Figure 21 suggests that the bands due to the  $\alpha$ -helix parts of the anti-mouse-IgG are particularly enhanced in the SERS spectrum. It seems likely that the  $\alpha$ -helix parts are closer to the surface of gold colloid particles.

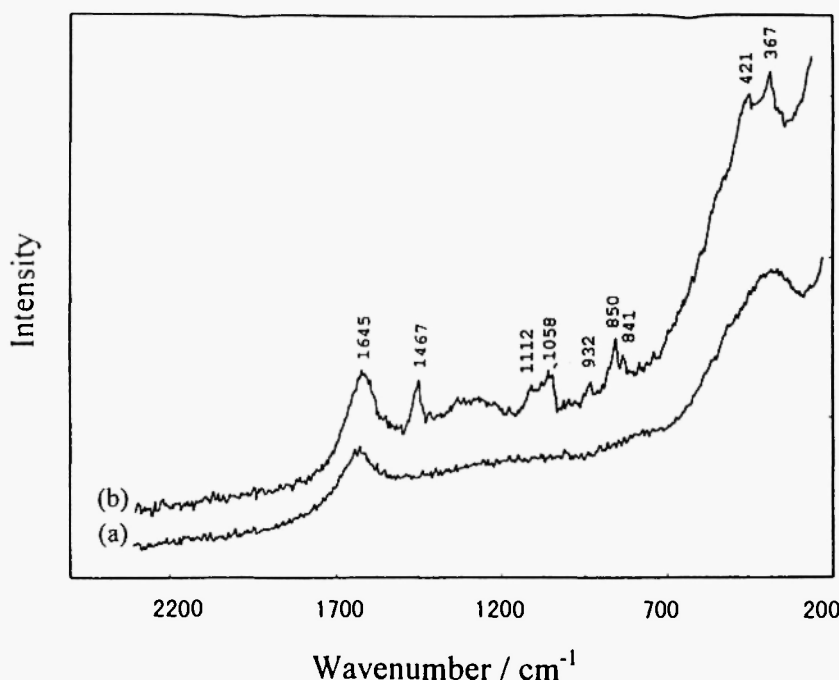
Figure 22 (a) shows a NIR SERS spectrum of anti-mouse IgG of  $10^{-10}$  M adsorbed on the gold colloid particles.<sup>31</sup> The Raman bands observed in the SERS spectrum of Figure 21 (b) disappear completely probably because the concentration of anti-mouse IgG was diluted by 100 times. Figure 22 (b) depicts a NIR-SERS spectrum of IgG-anti-IgG complex on the gold colloid

Table 3

Wavenumbers and assignments of SERS bands observed for anti-IgG on the gold colloid particles

SERS / cm <sup>-1</sup>	Assignments
1645	Amide I +water
1467	Trp
1261	Amide III
1112	Trp
1058	
925	Trp
880	Trp
850	Tyr
837	Tyr
672	Trp or C-S
549	
483	
417	Trp

particles.<sup>31</sup> Raman bands again appear, although they are weak. Note that the frequencies of those bands are very close to those of the Raman bands appeared in the spectrum shown in Figure 21. It seems that all the observed bands arise from the antibody part of IgG-anti-IgG complexes adsorbed on the gold colloid particles. In the system shown in Figure 20 the only antibody part can be adsorbed directly on the gold surface, giving the SERS signals. Free and bound antigen do not show significant Raman bands since free antigen molecules are blocked by BSA molecules and bound antigen molecules are adsorbed indirectly on the gold surface. It was concluded that the configuration of anti-mouse IgG is modified upon the reaction of antigen with anti-IgG on the gold colloid particles, emerging intense SERS signals.<sup>31</sup> In this way, the immune reaction on the gold surface can be detected by use of NIR SERS spectroscopy without any procedure for the B/F separation.



**Fig. 22:** (a) A NIR SERS spectrum of anti-mouse IgG of  $1.9 \times 10^{-10}$  M adsorbed on gold colloid particles. (b) A NIR SERS spectrum of IgG-anti-IgG complex on gold colloid particles. (Reproduced from ref. 31 with permission. Copyright (1998) John Wiley & Sons, Ltd.)

## REFERENCE

1. R. P. Van Duyne, In : *Chemical and Biochemical Applications of Lasers*, Vol. IV, ed. by C. B. Moore, Academic Press, New York, 1979, p. 101.
2. R. K. Chang and T. E. Furtak, Eds. *Surface-Enhanced Raman Scattering*, Plenum Press, New York, 1982.
3. T. M. Cotton, In : *Surface and Interfacial Aspects of Biomedical Polymers*, Vol. 2, ed. by J. Andrde, Plenum Press, New York, 1985, p 161.
4. M. Moskovits, *Rev. Mod. Phys.*, 57, 783 (1985).
5. E. Koglin and J. M. Sequareis, *Top. Curr. Chem.*, 134, 1(1986).

6. T. M. Cotton, In : *Spectroscopy of Surfaces*, ed. by R. J. H. Clark and R. E. Hester, John Wiley & Sons, Chichester, 1988, p 91.
7. R. F. Paisley and M. D. Morris, *Prog. Analyst. Spectrosc.*, 11, 111 (1988).
8. I. R. Nabiev, K. K. Sokolov, and M. Manfait, In : *Biomolecular Spectroscopy*, ed. by R. J. H. Clark and R. E. Hester, John Wiley & Sons, Chichester, 1993, p.267.
9. H. Fabian and P. Anzenbacher, *Vib. Spectrosc.*, 4, 125 (1993).
10. I. Nabiev and M. Manfait, In : *Biomedical Application of Spectroscopy*, ed. by R. J. H. Clark and R. E. Hester, John Wiley & Sons, Chichester, 1996, p .48.
11. I. R. Nabiev and V. A. Savchenko, *J. Raman Spectrosc.*, 14, 374 (1983).
12. S. J. Suh and J. A. Moskovits, *J. Am. Chem. Soc.*, 102, 7960 (1986).
13. D. Curley and O. Siiman, *Langmuir*, 4, 1021 (1988).
14. S. K. Kim, M. S. Kim, and S. W. Suh, *J. Raman Spectrosc.*, 18, 171 (1987).
15. R. E. Holt, and T. M. Cotton, *J. Am. Chem. Soc.*, 111, 2815 (1989).
16. T. M. Cotton, S. G. Schultz, and R. P. Van Duyne, *J. Am. Chem. Soc.*, 104, 6528 (1982).
17. R. Picorel, R. E Holt, T. M. Cotton, and M. Scibert, *J. Biol. Chem.*, 263, 4374 (1988).
18. K. Sokolov, P. Hodorchenko, A. Petukhov, I. Nabiev, G. Chumanov, and T. M. Cotton, *Appl. Spectrosc.*, 47, 515 (1993).
19. I. Nabiev, and M. Manfait, *Rev. Inst. Fr. Petr.*, 48, 261 (1993).
20. X. Dou, Y.M. Jung, H. Yamamoto, S. Doi, and Y. Ozaki, *Appl. Spectrosc.*, 53, 33 (1999).
21. X. Dou, Y.M. Jung, Z. Cao, and Y. Ozaki, *Appl. Spectrosc.*, in press.
22. K. Niki, and V. Brabec, *Biophys. Chem.*, 23, 63 (1985).
23. K. Kneipp, and J. Flemming, *J. Mol. Struct.*, 145, 173 (1986).
24. K. Kneipp, W. Pohle, and H. Fabian, *J. Mol. Struct.*, 244, 183 (1991).
25. N. R. Isola, D. L. Stokes, and T. Vo-Dinh, *Anal. Chem.*, 70, 1352 (1998).
26. T. Vo-Dinh, K. Houck, D.L Stokes, *Anal. Chem.*, 66, 3379 (1994).
27. X. Dou, T. Takama, Y. Yamaguchi, K. Hirai, H.Yamamoto, S. Doi, and Y. Ozaki, *Appl. Optics*, 37,759 (1998).
28. B. N. Rospendowski, J. M. Campbell, J. Reglinski, and W. E. Smith, *Eur. Biophys. J.*, 21, 257. (1992).

29. T. E. Rohr, T. M. Cotton, F. Ni, and P. Tarcha, *J. Anal. Biochem.*, 182, 388 (1989).
30. X. Dou, T. Takama, Y. Yamaguchi, H. Yamamoto, and Y. Ozaki, *Anal. Chem.*, 69, 1492 (1997).
31. X. Dou, Y. Yamaguchi, H. Yamamoto, S. Doi, and Y. Ozaki, *J. Raman Spectrosc.*, 29, 739 (1998).
32. H. Morjani, J. F. Riou, I. R. Nabiev, F. Lavelle, and M. Manfait, *Cancer Res.*, 53, 4784 (1993).
33. I. R. Nabiev, H. Morjani, and M. Manfait, *Eur. Biophys. J.*, 19, 311 (1991).
34. I. R. Nabiev, R. G. Efremov, and G. D. Chumanov, *Sov. Phys. Usp.*, 31, 241 (1988).
35. S. Nie and S. R. Emory, *Science*, 275, 1102 (1997).
36. K. Kneipp, H. Kneipp, G. Deinum, I. Itzkan, R. R. Dasari, and M. S. Feld, *Appl. Spectrosc.*, 52, 175 (1998).
37. J. A. Creighton, C. G. Blatchford, and M. G. Albrecht, *J. Chem. Soc. Faraday Trans II*, 75, 790 (1979).
38. P. C. Lee and D. Meisel, *J. Phys. Chem.*, 86, 3391 (1982).
39. E. J. Zeman and G. C. Slichtz, *J. Phys. Chem.* 91, 634 (1987).
40. A. Otto, I. Mrozek, H. Grabhorn, and W. Akemann, *J. Phys. Condens. Matter*, 4, 1143 (1992).
41. H. Xu, C. H. Tseng, T. J. Vickers, C. K. Mann, and J. B. Schelenoff, *Surf. Sci.* 311, L707 (1994).
42. K. Kneipp, R. R. Dasari, and Y. Wang, *Appl. Spectrosc.* 48, 951 (1994).
43. M. Takeda, R. E. S. Iavazzo, D. Garfinkel, I. H. Scheinberg, and J. T. Edsall, *J. Am. Chem. Soc.* 80, 3813 (1958).
44. K. Machida, A. Kagayama, Y. Saito, Y. Kuroda, and T. Uno, *Spectrochim. Acta*, Part A, 33A, 569 (1977).
45. K. Machida, A. Kagayama, Y. Saito, and T. Uno, *Spectrochim. Acta*, Part A, 34A, 909 (1978).
46. H. Susi and D. M. Byleer, *J. Mol. Struct.*, 63, 1 (1980).
47. J. Bandekar, L. Genzel, F. Kremer, and L. Santo, *Spectrochim. Acta*, Part A, 39A, 375 (1982).
48. A. Kourneberg, *DNA Replication*, Freeman, New York, 1980.
49. M. Singer and P. Berg, *Genes and Genomes*, University Science Books, Mill Valley, Calif., 1991.
50. J.-M. Sequaris, E. Koglin, and B. Malfoy, *FEBS Lett.*, 173, 95 (1984).
51. I. Nabiev, I. Chourpa, and M. Manfait, *J. Phys. Chem.*, 98, 1344 (1994).

52. A. T. Tu, in *Spectroscopy of Biological Systems*, ed. by R. J. H. Clark and R. E. Hester, Wiley, Chichester, 1986, p.47.
53. I. Harada and T. Takeuchi, *Spectroscopy of Biological Systems*, Chapter 3, Wiley, Chichester, 1986, p.113.
54. G. D. Chumanov, R. G. Efremov, and I. R. Nabiev, *J. Raman Spectrosc.*, 21, 43 (1990).
55. T. M. Cotton, J. M. Kim, and G. D. Chumanov, *J. Raman Spectrosc.*, 22, 729 (1991).
56. A. M. Ahern and R. L. Garrell, *Langmuir*, 7, 254 (1991).
57. E. S. Grabbe and R. P. Buck, *J. Electroanal. Chem.*, 308, 227 (1991).
58. P.C. Paoiinter and J.L. Koenig, *Biopolymers*, 14, 457 (1975).
59. M. Pezolet, M. Pigeon-Gosselin, and L. Coulombe, *Biochim. Biophys. Acta*, 453, 502 (1976).